(13) This bridge, not described in the literature, was built by one of us (R.H.C., 1973). It is quite similar to the General Radio 1615-A network. Signal generation and detection were by a PAR 124-A lock-in amplifier.
(14) Westphal, W. B. In "Dielectric Materials and Applications"; von Hippel, A., Ed.; Technology Press, MIT: Cambridge, MA, 1954.
(15) Mashimo, S.; Winsor, P., IV; Cole, R. H.; Matsuo, K.; Stockmayer, W. H. *Macromolecules* **1983**, *16*, 965.
(16) Helfand, E.; Wasserman, Z. R.; Weber, T. A.; Skolnick, J.; Runnels, J. H. *J. Chem. Phys.* **1981**, *75*, 4441.
(17) Maryott, A. A.; Smith, E. R. *Natl. Bur. Stand. (U.S.), Circ.* **1951**, *No. 514*.
(18) Block, H. *Adv. Polym. Sci.* **1979**, *33*, 93.
(19) Mark, J. E. *Acc. Chem. Res.* **1974**, *7*, 218.
(20) Chambers, S. C.; Fawcett, A. H. *Macromolecules* **1985**, *18*, 1710.
(21) Helfand, E. *Science (Washington, D.C.)* **1984**, *226*, 647.
(22) Bur, A. J.; Fetters, L. J. *Chem. Rev.* **1976**, *76*, 727.
(23) Matsuo, K., manuscript in preparation.

# Interactions of Sterically Stabilized Particles Suspended in a Polymer Solution

**Alice P. Gast***

*Department of Chemical Engineering, Stanford University, Stanford, California 94305, and Laboratoire d'Hydrodynamique et Mecanique Physique, E.S.P.C.I., 75231 Paris Cedex 05, France*

**Ludwik Leibler**

*Laboratoire de Physico-Chimie Macromoleculaire, E.S.P.C.I., 75231 Paris Cedex 05, France.*

*Received September 25, 1985*

ABSTRACT: We present a theory for the destabilization and restabilization of sterically stabilized colloidal particles suspended in a polymer solution. First, we calculate the structure of a layer of chains attached to a surface in equilibrium with a polymer solution. We then determine the concentration profiles of the free polymer chains near the anchored layer via a self-consistent field theory. There is a depletion of mobile chains near the steric layer similar to the depletion layer next to a hard wall. The existence of a depletion layer produces a weak attractive interaction between colloidal particles. We show typical concentration profiles and interaction energies and we discuss how colloidal stability depends on the surface density of anchored chains and the concentration of free chains.

## 1. Introduction

The weak flocculation of colloidal particles induced by nonadsorbing polymers has been studied experimentally for many aqueous[1-4] and nonaqueous[5,6] suspensions. Several theories attribute this flocculation to a depletion of polymer segments around a hard particle.[7-10] The gradient in polymer concentration near the particles leads to a positive surface energy and hence an attraction between particles. The suspension tends to minimize the volume inaccesible to the polymer by forming weak clusters. Addition of this depletion-layer attractive potential energy to a hard-sphere or electrostatic repulsion allows satisfactory prediction of the weak flocculation of several suspensions.[3,4,6,10,11] Additionally, the existence of the depletion layer for flat plates has been confirmed by optical experiments.[12]

Many suspensions are not made up of hard spheres but comprise particles protected from flocculation by a layer of polymer chains attached to their surfaces. This way of protecting particles is known as steric stabilization and has been studied extensively in experiment and theory.[13] The polymer chains in the dense steric layer repel one another and are stretched from their free coil conformation, thus providing a repulsion between particles whenever two steric layers are forced to overlap. This repulsion may be of a range and magnitude sufficient to prevent flocculation due to London-van der Waals attractions.

When sterically stabilized particles are suspended in a polymer solution, the interactions are complicated by the repulsion between anchored and free chains. Indeed, several experimental studies[1,5,13] show that low concentrations of free polymer can cause a weak flocculation, while at higher concentrations the system remains stable. The goal of this paper is to present a mechanism for this flocculation and restabilization and to relate the mechanism to the structure of the anchored layer and the free polymer concentration profile.

de Gennes[14] has recently studied the interactions between a solution of mobile chains and a layer of chains anchored to a single wall, focusing on the conformations of the attached chains. He found that the structure of the anchored layer can be classified by several regimes depending on its surface density, molecular weight, and the concentration and molecular weight of the free chains. In order to investigate the interactions between sterically stabilized particles suspended in a polymer solution, one must determine the concentration profile of free chains between two steric layers. The regimes defined by de Gennes for the structure of a single steric layer suggest a mechanism for the destabilization and restabilization of polymer-coated colloidal particles suspended in a polymer solution. We have proposed[15] that the destabilization occurs at low free polymer concentrations where a depletion layer forms. We predicted equilibrium restabilization as the free polymer solution concentration aproaches that in the anchored layer and the depletion layer is supressed. In this paper we present detailed self-consistent field calculations of the unattached polymer concentration profiles and the resulting interaction potential between particles, thus determining stable and unstable regimes in polymer concentration and anchored chain surface density.

The paper is organized as follows. We begin in section 2 with a mean-field calculation of the structure of a single steric layer in equilibrium with a free polymer solution. In section 3 we present a self-consistent field calculation

© 1986 American Chemical Society

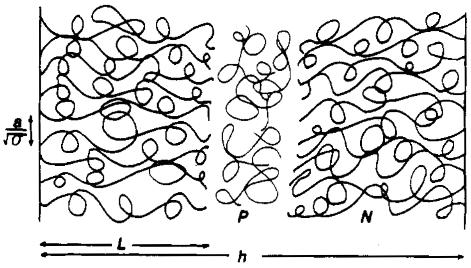

**Figure 1.** Illustration of two-plate geometry. Each plate carries a dense layer of terminally anchored polymer chains of $N$ monomers of dimensionless surface density $\sigma$. The plates are separated by a distance $h$ and immersed in a solution of polymer molecules of $P$ monomers.

of the free polymer concentration profile between two steric layers. We then derive the interaction potential energy resulting from the free polymer concentration gradient. This calculation is a basis for our discussion of colloidal stability presented in section 4.

## 2. Structure of a Steric Layer Equilibrated with a Polymer Solution

We consider a solution of mobile chains of $P$ monomers in a good solvent at a volume fraction $\phi_o$ between two parallel plates separated by a distance $h$. Each plate has a steric layer of chains of $N$ monomers ($N > P$) of the same composition as the $P$ chains attached by one end only at a dimensionless surface density $\sigma$. The average distance between anchor points is $a/\sigma^{1/2}$, where $a$ is the monomer size. We consider situations where the surface density is sufficient for the anchored chains to be strongly overlapping, as found with many sterically stabilized suspensions.[13] The geometry of this system is illustrated in Figure 1.

The problem of the conformations of a single steric layer has been treated in ref 14 with a scaling theory. Here we introduce a simple mean-field calculation that forms the basis for our detailed study of mobile chain concentration profiles. We derive the layer thickness $L$ and its average volume fraction $\phi_N$ by calculating the free energy of a steric layer in equilibrium with a polymer solution. The dominant contributions to the free energy inside the steric layer are the elastic deformation energy of extended $N$ chains, the excluded-volume repulsion between monomers, and the translational entropy of free chains. Thus we write the free energy density as

$$\frac{E}{kT} = \frac{3}{2}\left(\frac{\sigma a}{L}\right)\frac{L^2}{R^2} + \frac{\upsilon}{2}(\phi_N + \phi_P)^2 + \frac{\phi_P}{P} \ln \phi_P \qquad (1)$$

where $R^2 = Na^2$ is the unperturbed end-to-end distance for $N$ chains and $\upsilon = (1 - 2\chi)$ is the dimensionless excluded-volume parameter expressed in terms of the Flory $\chi$ parameter. Outside the anchored layer we denote the $P$ chain volume fraction by $\phi_o$, and the free energy density takes the simple form $E/kT = (\upsilon/2)\phi_o^2 + (\phi_o/P) \ln \phi_o$. Equilibrium between the bulk solution and the steric layer requires that the chemical potential of the solvent and free polymer chains are equal. This is equivalent to equating the exchange potentials, $\mu = \partial F/\partial\phi_P$, and the osmotic pressures, $\Pi = \phi_N \partial F/\partial\phi_N + \phi_P\, \partial F/\partial\phi_P - F$, inside and outside the steric layer. These equalities yield two equations

$$\upsilon(\phi_N + \phi_i) + \frac{1}{P} \ln \phi_i = \upsilon\phi_o + \frac{1}{P} \ln \phi_o \qquad (2)$$

and

$$\frac{\upsilon}{2}(\phi_N + \phi_i)^2 - 3\frac{\sigma^2}{\phi_N} + \frac{\phi_2}{P} = \frac{\upsilon}{2}\phi_o^2 + \frac{\phi_o}{P} \qquad (3)$$

defining the average volume fraction of $N$ chains, $\phi_N$, and $P$ chains inside the anchored layer, $\phi_i$, in terms of the average bulk volume fraction of $P$ chains outside the layer, $\phi_o$.

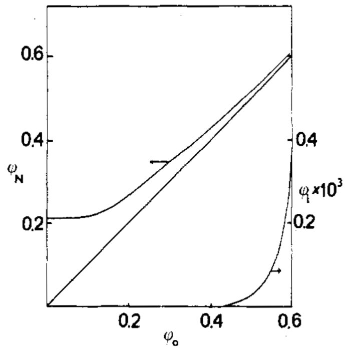

**Figure 2.** The volume fraction of anchored chains, $\phi_N$, and mobile chains, $\phi_i$, inside the steric layer as a function of the external solution concentration $\phi_o$. Here $N = 5 \times 10^3$, $P = 5 \times 10^2$, $\upsilon = 1$, and $\sigma = 0.04$.

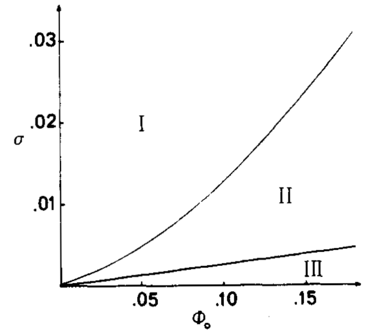

**Figure 3.** The regimes of steric-layer structure on a plot of surface density $\sigma$ vs. external solution concentration $\phi_o$. Regime I is the $\sigma$-dominated regime, regime II the $\phi_o$-dominated regime, and regime III the penetration regime described in the text. Here $N = 5 \times 10^3$, $P = 5 \times 10^2$, and $\upsilon = 1$.

In a pure solvent, $\phi_o = 0$, the anchored chains are extended from their coil configuration, and the concentration is nearly constant over most of the steric layer. The concentration and thickness of the layer depend only on the surface density as $\phi_N = (6/\upsilon)^{1/3}\sigma^{2/3}$ and $L = Na(\upsilon\sigma/6)^{1/3}$. At finite $\phi_o$, the relations 2 and 3 yield a simple general expression for $\phi_N$

$$\phi_N = \phi_o + \frac{1}{\upsilon P} \ln \frac{\phi_o}{\phi_i} - \phi_i \qquad (4)$$

in terms of the average $P$ chain concentration inside and outside the anchored layer. Thus, the equilibrium condition (3) can be solved explicitly for the partitioning of free chains between the bulk solution and steric layer as shown, for example, in Figure 2. We note that at low $\phi_o$ the steric layer concentration is only weakly dependent on the presence of the free polymers; however, as the free polymer concentration increases, $\phi_N$ approaches $\phi_o$. The average concentration of $P$ chains penetrating the steric layer, $\phi_2$, remains small as shown in Figure 2. These two types of steric layer behavior are representative of general regimes of anchored layer structure (Figure 3).

At low free polymer concentrations, $\phi_o < (6/\upsilon)^{1/3}\sigma^{2/3}$, the anchored chain properties are dominated by their surface density with the steric layer concentration

$$\phi_N^{\mathrm{I}} = (6/\upsilon)^{1/3}\sigma^{2/3} + \phi_o \qquad (5)$$

only slightly different than it was in a pure solvent. The steric layer thickness is approximately the same as the pure solvent case, $L^{\mathrm{I}} = Na(\upsilon\sigma/6)^{1/3}$. Here the penetration of free chains into the anchored layer is exponentially small

$$\phi_1^{\mathrm{I}} \simeq \phi_o \exp(-6^{1/3}v^{2/3}\sigma^{2/3}P) \qquad (6)$$

depending both on the molecular weight, $P$, and on $\sigma$. This is denoted the $\sigma$-dominated regime I in Figure 3. The lower limit of $\sigma$ domination and negligible penetration is $\sigma = 2/(3^{1/2}vP^{3/2})$, normally, very low due to the strong dependence on $P$.

As $\phi_o$ is increased above $(6/v)^{1/3}\sigma^{2/3}$, the steric layer contracts under the osmotic pressure of the solution until its concentration

$$\phi_N^{\mathrm{II}} = \phi_o + \frac{3}{v}\frac{\sigma^2}{\phi_o^2} \qquad (7)$$

just exceeds that of the solution. Now the anchored layer thickness is inversely proportional to the solution concentration: $L^{\mathrm{II}} = Na\sigma/\phi_o$. This is the $\phi_o$-dominated regime II in Figure 3. In this regime the penetration into the layer remains small, the average volume fraction inside given by

$$\phi_2^{\mathrm{II}} = \phi_o \exp(-3\sigma^2 P/\phi_o^2) \qquad (8)$$

The crossover between I and II occurs when $\phi_o = (6/v)^{1/3}\sigma^{2/3}$.

Increasing $\phi_o$ further causes increasing penetration into and compression of the steric layer. Below a surface density $\sigma = \phi_o/(3P)^{1/2}$, substantial penetration occurs such that the volume fraction inside

$$\phi_i^{\mathrm{III}} = \phi_o(1 - (3P)^{1/2}\sigma/\phi_o) \qquad (9)$$

is no longer small. In this regime III, the anchored chain concentration is independent of the free polymer concentration once again and is linear in $\sigma$: $\phi_N^{\mathrm{III}} = (3P)^{1/2}\sigma$. Likewise the thickness $L = Na/(3P)^{1/2}$ is independent of $\sigma$. This regime may be of some importance for small $P$ chains; however, in most applications the limiting surface density will be very small, e.g., Figure 3.

In summary, for most practical applications there are two important regimes for steric layer thickness and density. In the first regime, the steric layer surface density dominates its properties, the free chains providing only a perturbation. In the second regime, the steric layer density is nearly equal to that of the polymer solution. In both these regimes there is little penetration of free polymer into the steric layer. Now we can proceed to calculate the more detailed free polymer concentration profile.

## 3. Free Polymer Concentration Profile and Interaction Potential Energy

We follow the self-consistent field approach of Edwards[16] to calculate the concentration profile of free polymers confined between layers of anchored chains. The self-consistent field theory describes the configurational probability distribution of a polymer chain by a diffusion equation forced by a self-consistent field representing the inter- and intramolecular excluded-volume interactions between polymer segments. The complete coupled equations presented in the Appendix can be solved numerically for any anchored ($N$) chain and free ($P$) chain profiles. We illustrate the calculation for chemically identical $N$ and $P$ chains where the surface density is high enough to prevent large amounts of penetration as described above. In this regime, as shown by self-consistent field theory[16] and scaling theory[14] calculations, the $N$ chain concentration is constant over most of the layer thickness $L$. Thus we calculate the free chain concentration profile by solving one differential equation wherein we approximate the $N$ chain profile as a constant step of height $\phi_N$ and width $L$.

The equation for the $P$ chain probability distribution is then

$$\left[\frac{\partial}{\partial s} - \frac{a^2}{6}\frac{\partial^2}{\partial z^2} + \partial(\phi_P(z) + \phi_N(H(z-L) + H(z-h+L)))\right]\mathrm{G}_P(z, z', s) = \delta(z - z_0)\delta(s) \qquad (10)$$

with $G_P = 0$ at $z = 0$ and $h$ and $\partial G_P/\partial z = 0$ at $z = h/2$, where $H(z)$ is the Heaviside function and $s$ represents the step along the chain. The $\delta$ functions, $\delta(z - z_o)\delta(s)$, provide the initial condition with the chain beginning at $z_o$. The concentration profile is found by integrating $G_P$ over the length of the chain as

$$\phi_P(z) = \int_0^P \mathrm{d}s\, \frac{G_P(z, z', s)G_P(z'', z, P - s)\,\mathrm{d}z''}{G_P(z'', z, P)\,\mathrm{d}z''} \qquad (11)$$

Expanding $G_P(z, z', s)$ as a series of eigenfunctions and taking the limit of long polymer chains, ($\phi_o P \gg 1$), we find the concentration profile dominated by the first eigenvalue $\epsilon_o$

$$G_P(z, z', P) = \psi(z)\psi(z')e^{-\epsilon_o P} \qquad (12)$$

with the renormalization constant defined such that the volume fraction is simply related to the wavefunction solution to (10) by $\phi_P(z) = \psi^2(z)$.

We now have a Schrödinger-like equation for a trajectory in a one-dimensional box with a self-constant field $v\psi^2(z)$

$$-\frac{a^2}{6}\frac{\partial^2\psi}{\partial z^2} + v(\psi^2(z) + \phi_N(H(z-L) + H(z-h+L)))\psi(z) = \epsilon_o\psi(z) \qquad (13)$$

with boundary conditions $\psi(z) = 0$ at $z = 0$ and h and $\partial\psi/\partial z = 0$ at $z = h/2$. At large separations, far from the wall, we must recover the bulk concentration $\phi_o \equiv \psi_o^2$, thus fixing the eigenvalue $\epsilon_o = v\psi_o^2 = v\phi_o$. When the equation is divided into two regimes outside (I) and inside (II) the anchored layer and written in dimensionless form

$$\frac{\partial^2\psi_{\mathrm{I}}}{\partial z^2} + \frac{1}{\xi^2}\left(1 - \frac{\psi_{\mathrm{I}}^2(z)}{\psi_o^2}\right)\psi_{\mathrm{I}}(z) = 0 \qquad (14)$$

and

$$\frac{\partial^2\psi_{\mathrm{II}}}{\partial z^2} + \frac{1}{\xi^2}\left(1 - \frac{\xi^2}{\xi_b^2} - \frac{\psi_{\mathrm{II}}^2(z)}{\psi_o^2}\right)\psi_{\mathrm{II}}(z) = 0 \qquad (15)$$

with matching conditions that $\psi_{\mathrm{I}} = \psi_{\mathrm{II}}$ and $\partial\psi_{\mathrm{I}}/\partial z = \partial\psi_{\mathrm{II}}/\partial z$ at $z = L$ or $h - L$ naturally introduces two length scales $\xi = a/(6v\phi_o)^{1/2}$ and $\xi_b = a/(6v\phi_N)^{1/2}$, the correlation lengths or the free polymer and anchored layer respectively. We note that (14) is the same equation describing depletion layers between hard walls[9] except for the boundary condition at $z = L, h - L$.

Integrating (14) once and applying symmetry conditions, we obtain

$$\frac{1}{2\psi_o^2}\left(\frac{\partial\psi_{\mathrm{I}}}{\partial z}\right)^2 = \frac{1}{\xi^2}\left[\frac{\psi_{\mathrm{I}}^4(z) - \psi_c^4}{4\psi_o^4} - \frac{\psi_{\mathrm{I}}^2(z) - \psi_c^2}{2\psi_o^2}\right] \qquad (16)$$

where $\psi_c$ is the value of $\psi(z)$ at $z = h/2$ where $\partial\psi/\partial z = 0$. Likewise we integrate (15) once applying matching conditions at $z = L$, providing

$$\frac{1}{2\psi_o^2}\left(\frac{\partial\psi_{\mathrm{II}}}{\partial z}\right)^2 = \frac{1}{\xi^2}\left[\frac{\psi_{\mathrm{II}}^4-\psi_c^4}{4\psi_o^4}-\frac{\psi_{\mathrm{II}}^2-\psi_c^2}{2\psi_o^2}+\frac{\xi^2}{\xi_b^2}\,\frac{\psi_{\mathrm{II}}^2(z)-\psi^2(L)}{2\psi_o^2}\right] \quad (17)$$

where $\psi^2(L)$ is the concentration at the edge of the steric layer. We solve these equations for the maximum concentration between the plates, $\phi_c = \psi_c^2$, from integration of (16) as

$$\frac{1}{(1-X^2)^{1/2}}\int_{\Phi}^{\Pi/2}\frac{\mathrm{d}u}{(1-k^2\sin^2 u)^{1/2}} = (1+k^2)^{1/2}[K(k^2)-F(k^2/\Phi)] = \frac{h/2-L}{\xi} \quad (18)$$

where $K(k^2)$ and $F(k^2/\Phi)$ are elliptic integrals[17] and $k^2 = X^2/(1-X^2)$ with $X^2 = \psi_c^2/2\psi_o^2 = \phi_c/2\phi_o$. The lower limit of the integral $\Phi = \arcsin\,(\psi(L)/\psi_c)$ depends on the matching concentration $\phi(L)$ given implicitly by

$$\int_0^{Y(L)}\frac{\mathrm{d}Y}{(Y^4-Y^2-X^2-X^4+(\xi^2/\xi_b^2)(Y^2-Y^2(L)))^{1/2}} = \frac{L}{\xi} \quad (19)$$

where $Y^2 = \psi^2/2\psi_o^2 = \phi/2\phi_o$ and $Y^2(L) = \psi^2(L)/2\psi_o^2$. After finding $\phi(L)$ and $\phi_c$ as functions of $L$, $h$, and $\xi/\xi_b$, (18) and (19) are resolved for the concentration profile $\phi(z)$ by integration to $z < h/2$ and $u < \Pi/2$ in (18) and $z < L$ and $Y < Y(L)$ in (19). Typical profiles are presented in section 4.

The interaction potential energy per chain between two plates may be obtained from the concentration profile via the Cahn–Hilliard theory of interfaces[18]

$$V_A = \frac{a^2}{\sigma}\int_0^h G\{\psi(z)\}\,\mathrm{d}z \quad (20)$$

where the energy density functional $G\{\psi(z)\}$ includes contributions from spatial variations of concentration $\phi(z) = \psi^2(z)$

$$G\{\psi(z)\} = \frac{a^2}{6}\left(\frac{\partial\psi}{\partial z}\right)^2 + F\{\phi_N,\phi(z)\} - \mu_o\phi(z) + \Pi_o \quad (21)$$

the free energy density $F$, exchange potential $\mu_o$, and osmotic pressure of a homogeneous solution. The last three terms in (21) represent the free energy needed to create a unit volume at a composition $\phi(z)$ from a solution of osmotic pressure, $\Pi_o = \mu_o\phi_o - F_o$, and exchange potential $\mu_o = \partial F/\partial\phi_o = v\phi_o$. We note that (13) is the Euler–Lagrange equation minimizing the interaction energy $V_A$.

We combine this attraction with the repulsion between steric layers modeled as the sum of elastic and mixing energies

$$\frac{V_R}{kT} = N\left(\frac{3}{2}\,\frac{\sigma a}{(h/2)}\,\frac{(h/2)^2}{R^2} + \frac{v}{2}\,\frac{N^2a^2\sigma^2}{(h/2)^2}\right) \quad (22)$$

for $h < 2L$. Now we are able to calculate concentration profiles and interaction energies and distinguish stable and unstable conditions for colloidal particles.

## 4. Results and Discussion

We present free polymer concentration profiles for several bulk concentrations and anchored chain densities at fixed chain lengths of $N = 5 \times 10^3$ and $P = 5 \times 10^2$. The excluded-volume parameter $v = 1$ corresponds to an athermal solvent in all our examples. The plate–plate interaction potential resulting from these profiles provides a criterion for a stability diagram. The two regimes of low and high free polymer concentration correspond to regimes of instability and stability for colloidal suspensions.

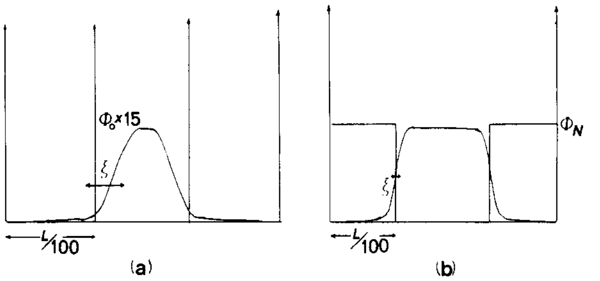

**Figure 4.** Plots of free chain concentration profiles between sterically stabilized plates superimposed on the rescaled ($L/100$) anchored chain step-function profiles. In this situation the anchored chain dimensionless surface density is $\sigma = 0.04$, the excluded volume parameter $v = 1$, and the chains are $N = 5 \times 10^3$ monomers long. The free chains, of $P = 5 \times 10^2$ monomers, are at bulk volume fractions of (a) $\phi_o = 0.02$ and (b) $\phi_o = 0.30$. The correlation length, $\xi$, is indicated on the profile.

**Low Free Polymer Concentrations: Regime I.** At free polymer concentrations below $\phi = (6/v)^{1/3}\sigma^{2/3}$ the dense anchored layer is only slightly perturbed by the free polymer chains (eq 5). Solution of (18) and (19) yields a concentration profile having a depletion layer outside the anchored layer analogous to the situation near a hard wall[9] except for the slight penetrability of the steric layer. A typical concentration profile is illustrated in Figure 4a. The concentration outside of the steric layer decays on a length we define as the depletion layer thickness

$$d \simeq \pi\xi(1-\xi_b/\xi)/2 \quad (23)$$

given in terms of the correlation lengths in the solution, $\xi$, and in the anchored layer, $\xi_b$. While the average penetration into the anchored layer remains exponentially small, the concentration of free polymer at the steric layer–solution interface does not. It is this concentration given approximately by

$$\phi(L) \simeq \phi_o\frac{\xi_b^2}{\xi^2}\left(\frac{\phi_c}{\phi_o}-\frac{\phi_c^2}{2\phi_o^2}-\frac{\xi^2}{L^2}\right) \quad (24)$$

or for $h > 2(L+d)$, $\phi(L) \simeq (\phi_o/2)(\xi_b/\xi)^2$, that determines the boundary conditions for the solution of (18) for the profile between steric layers and represents the major difference between this problem and the one handled in ref 9. The free polymer concentration decays rapidly over a length $\xi_b$ to small average in (6) decaying again to zero near the wall.

The concentration gradient in the depletion layer produces a surface energy at the steric layer–solution interface, yielding an attraction between plates similar to that between hard plates.[9] The interaction potential energy between two plates resulting from the concentration profile in Figure 4a is presented in Figure 5a. As the free chain concentration increases and the depletion layer diminishes, the range and magnitude of the attraction also decrease. In terms of the correlation lengths, the magnitude decreases as $\xi(\phi_o)$ approaches $\xi_b(\phi_N)$ as

$$V_A \simeq kT\phi_o^{3/2}(1-\xi_b/\xi) \quad (25)$$

and the range equals 2 times the sum of the depletion layer and steric layer ($2L + \pi\xi(1-\xi_b/\xi)$).

**High Free Polymer Concentration: Regime II.** In the more concentrated regime, $\phi_o > (6/v)^{1/3}\sigma^{2/3}$, the an-

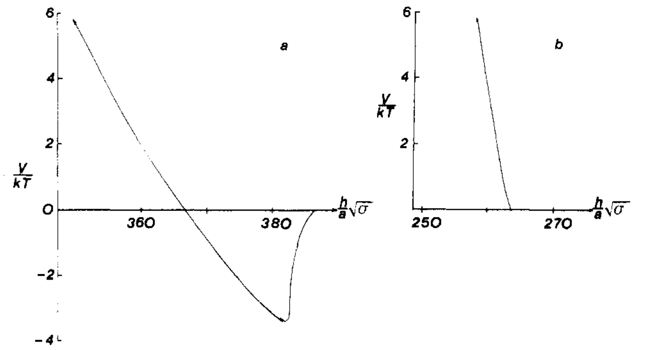

**Figure 5.** The interaction potential energy between two sterically stabilized flat plates immersed in a polymer solution. The conditions correspond to those in Figure 3 (a) $\phi_o = 0.02$ and (b) $\phi_o = 0.30$.

chored layer contracts under the osmotic pressure of the solution until its concentration just exceeds that of the solution (eq 7). Due to this adjustment and an increasing free polymer penetration, the total polymer concentration is nearly constant throughout the fluid. Thus, the attraction due to depletion layer effects becomes negligible. In terms of (23) the free and anchored chain concentrations are so close that $\xi \simeq \xi_b$ and the depletion layer diminishes as illustrated in Figure 4b. In the absence of other interactions the net potential is the repulsion between two compressed steric layers shown in Figure 5b.

The contraction of the steric layers may reduce a particle's protection against London–van der Waals attractions. If the steric layers remain sufficiently extended to avoid this type of flocculation, the suspension will be thermodynamically stable at these moderate polymer concentrations. This may explain the observation of stable suspensions at moderate polymer concentrations in systems flocculated at lower $\phi_o$.

Qualitatively, the mean-field picture of equilibrium destabilization and restabilization of suspensions by polymer solutions is correct. However, the mean-field theory does not account completely for concentration fluctuations in semidilute solutions, and some of its quantitative predictions should be modified by a more proper scaling analysis.[19] For example, in the depletion layer regime, the thickness of the depletion zone near the steric layer has the thickness of about $\xi(1 - \xi_b/\xi)$, but the correlation lengths $\xi(\xi_b)$ should vary as $\phi_o^{-3/4}(\phi_N^{-3/4})$ rather than $\phi_o^{-1/2}(\phi_N^{-1/2})$. On the other hand, the above self-consistent calculation based on a Flory–de Gennes type argument correctly determines the equilibrium anchored chain layer thickness and also the crossover concentration for disappearence of depletion layer attraction. The interfacial energy $\gamma$ associated with the depletion layer scales as $(kT/\xi^3)(1 - \xi/\xi_b)$, which for low concentrations $\phi_o$ yields the same dependence on concentration, $\gamma \sim \phi_o^{3/2}$, as the mean-field theory. However, mean-field calculations of forces both for steric repulsion and depletion-layer attraction give only approximate concentration dependence.

While our theory is only rigorous for $N > P$ we expect the depletion-layer mechanism to remain valid for $N < P$. As $P$ increases, penetration into the steric layer will decrease. Penetration will only occur at elevated concentrations if at all, and the details of the partitioning and steric layer structure remain to be determined.

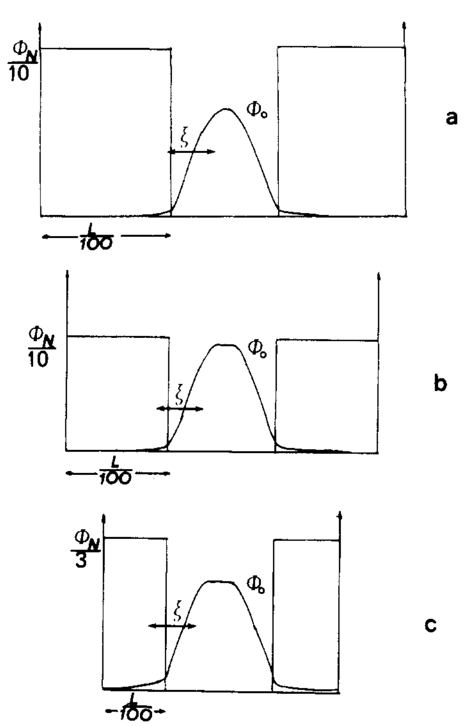

**Figure 6.** The effect of anchored chain surface density on the free chain concentration profiles between sterically stabilized plates. Again the profiles are superimposed on the rescaled $(L/100)$ anchored chain step-function profiles. The molecular weights are constant with $N = 5 \times 10^3$ and $P = 5 \times 10^2$, $v = 1$, and the free polymer volume fraction is $\phi_o = 0.02$. The dimensionless surface densities and corresponding average surface area per chain are (a) $\sigma = 0.08$, area = 450 Å$^2$; (b) $\sigma = 0.04$, area = 900 Å$^2$; (c) $\sigma$ 0.01, area = 3,600 Å$^2$. The correlation length, $\xi$, is indicated on the profile.

**Effect of Surface Density.** The concentration profiles between two plates at a constant free polymer concentration ($\phi_o < (6/v)^{1/3}\sigma^{2/3}$) and three different anchored chain surface densities are presented in Figure 6. Two effects are present on increasing $\sigma$. First, the steric-layer thickness and concentration increase with $\sigma$ as $L \sim \sigma^{1/3}$ and $\phi_N \sim \sigma^{2/3}$, increasing the range and magnitude of the steric repulsion. Increasing $\sigma$ also affects the depletion layer by reducing the free chain penetration into the anchored layer. As the penetration decreases, the free chains create a more profound and wider depletion layer and hence a greater attractive energy. This decrease in protection against depletion-layer flocculation upon increasing $\sigma$ is contrary to usual considerations for steric stabilization against London–van der Waals attraction.

**Colloidal Stability Considerations.** The above calculations of interaction potentials between two plates must be related to particle–particle interactions. For spherical particles this is readily accomplished via the Derjaguin approximation[20] or from a calculation of the lens-shaped volume of two overlapping spherical depletion layers.[8] These are reliable approaches provided that the steric layers are smaller than the particles. Very long anchored chains or more complicated geometries may require a geometry-specific calculation.

The weak flocculation of colloidal suspensions occurs when the attractive well reaches a depth of approximately $3kT$.[3,11] Thus we can determine limits of stability in the absence of other forces in terms of anchored chain surface density and free polymer concentration as shown for flat plates in Figure 7. The weak flocculation is reversible and can be described as a pseudo-phase-transition. Depending on the range and magnitude of the attraction, the flocculated phase will have fluid or solid properties.[4,11] At a second threshold of approximately $20kT$,[21] the particles no longer form equilibrium phases but rather create open low-density structures. Therefore knowledge of the interaction potential between particles provides important information for the prediction of the nature of a colloidal suspension.

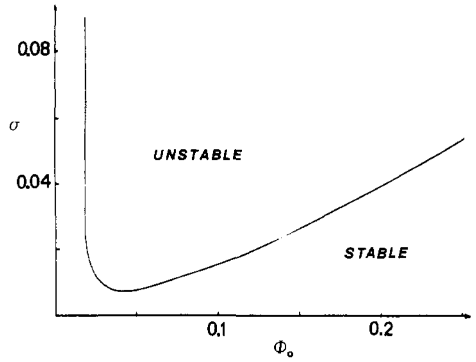

**Figure 7.** A plot showing regions of stability and instability for two sterically stabilized plates immersed in a polymer solution as a function of surface density $\sigma$ of anchored chains and free polymer concentration $\phi_o$. The curve represents the point where the attractive interaction potential reaches a magnitude of approximately $-3.5kT$. The low concentration regime is stable and at higher concentrations another stable regime is predicted. This diagram only accounts for attractions due to dissolved polymer and does not include London–van der Waals attractions.

In conclusion, we have presented a mechanism for the weak flocculation and restabilization of sterically stabilized suspensions in polymer solutions. Our calculations are based on a mean-field analysis of the interactions between attached and mobile chains. We developed a self-consistent field theory to determine free chain concentration profiles and plate–plate interaction energies. The formation of a depletion layer outside the protective polymer layer causes weak flocculation. When the free polymer solution concentration reaches a threshold, $\phi_o = (6/v)^{1/3}\sigma^{2/3}$, the concentration of the protective layer remains approximately equal to that of the solution; thus the depletion layer disappears and the suspension is stable. These stable and unstable regimes are well characterized in terms of the correlation lengths for the free polymer solution and anchored chains.

**Acknowledgment.** We thank R. Audebert, P.-G. de Gennes, J. F. Joanny, P. Pincus, and M. V. Tirrell for stimulating discussions on this subject. A.P.G. gratefully acknowledges the support of the NSF–NATO postdoctoral fellowship.

## Appendix

We present the complete coupled self-consistent field equations to be solved numerically for the concentration profiles of any anchored polymer chains in a steric layer interacting with any free chains in solution. Following Dolan and Edwards,[22] we write the diffusion equations for the anchored $N$ chains

$$\left[\frac{\partial}{\partial s} - \frac{a_N^2}{6}\nabla^2 + v_{NN}\phi_N(\mathbf{r}) + v_{NP}\phi_P(\mathbf{r})\right]G_N(\mathbf{r}, \mathbf{r}') = \sigma^{1/2}\delta(\mathbf{r} \pm \mathbf{x} + \mathbf{y})\delta(s) \quad \text{(A.1)}$$

and for the free $P$ chains

$$\left[\frac{\partial}{\partial s} - \frac{a_P^2}{6}\nabla^2 + v_{NP}\phi_N(\mathbf{r}) + v_{PP}\phi_P(\mathbf{r})\right]G_P(\mathbf{r}, \mathbf{r}') = \delta(\mathbf{r} - \mathbf{r}_o)\delta(s) \quad \text{(A.2)}$$

where $a_N$ and $a_P$ are the monomer lengths and $v_{NN}$, $v_{PP}$, and $v_{NP}$ are the dimensionless excluded-volume parameters for the $N$–$N$, $P$–$P$, and $N$–$P$ interactions. The source terms on the right-hand sides provide the initial conditions that the $N$ chains must begin at the plate surfaces $\mathbf{r} = \pm(\mathbf{x} + \mathbf{y})$ and the $P$ chains begin somewhere in the solution $\mathbf{r}_o$. The boundary conditions are no flux through the walls $G_P = G_N = 0$ at $\mathbf{r} = \pm(\mathbf{x} + \mathbf{y})$ and that $G_N \rightarrow 0$ and $G_P = 1$ as $\mathbf{r} \rightarrow \infty$. These equations are coupled through the excluded-volume interactions between $P$ and $N$ chains $v_{NP}\phi(\mathbf{r})$. The density profiles $\phi(r)$ are found from the probability distribution by

$$\phi(r) = \int_0^l \mathrm{d}s \left[\frac{G(r, r', s)\int G(r'', r, l - s)\,\mathrm{d}r''}{\int G(r'', r, l)\,\mathrm{d}r''}\right] \quad \text{(A.3)}$$

for both $P$ and $N$ chains with $l = P$ or $l = N$, respectively. These three equations allow a self-consistent numerical calculation of any free and anchored chain concentration profiles.

## References and Notes

(1) Cowell, C.; Lin-in-on, R.; Vincent, B. *J. Chem. Soc., Faraday Trans. 1*, **1978**, *74*, 337.
(2) Sperry, P. R.; Hopfenberg, H. B.; Thomas, N. L., *J. Colloid Interface Sci.* **1981**, *82*, 62.
(3) Sperry, P. R. *J. Colloid Interface Sci.* **1982**, *87*, 375; **1984**, *99*, 97.
(4) Gast, A. P.; Russel, W. B.; Hall, C. K. *J. Colloid Interface Sci.*, in press.
(5) Clarke, J.; Vincent, B. *J. Colloid Interface Sci.* **1981**, *82*, 208; *J. Chem. Soc., Faraday Trans. 1* **1981**, *77*, 1831.
(6) DeHek, H.; Vrij, A. *J. Colloid Interface Sci.* **1981**, *84*, 409.
(7) Asukura, S.; Oosawa, F. *J. Chem. Phys.* **1954**, *22*, 1255; *J. Polym. Sci.* **1958**, *33*, 183.
(8) Vrij, A. *Pure Appl. Chem.* **1976**, *48*, 471.
(9) Joanny, J. F.; Leibler, L.; de Gennes, P.-G. *J. Polym. Sci., Polym. Phys. Ed.* **1979**, *17*, 1073.
(10) Scheutjens, J. M. H. M.; Fleer, G. J. *Adv. Colloid Interface Sci.* **1982**, *16*, 361.
(11) Gast, A. P.; Hall, C. K.; Russel, W. B. *J. Colloid Interface Sci.* **1983**, *96*, 251; *Faraday Discuss. Chem. Soc.* **1983**, *76*, 189.
(12) Allain, C.; Ausserre, D.; Rondelez, F. *Phys. Rev. Lett.* **1982**, *49*, 1694.
(13) Napper, D. H. "Polymeric Stabilization of Colloidal Dispersions"; Academic Press: London, 1983.
(14) de Gennes, P.-G. *Macromolecules* **1980**, *13*, 1069.
(15) Gast, A. P.; Leibler, L. *J. Chem. Phys. Lett.* **1985**, *89* (19), 3947.
(16) Edwards, S. F. *Proc. Phys. Soc.* **1965**, *85*, 613.
(17) Gradshtein, I. S.; Ryznik, I. M. "Tables of Integrals Series and Products"; Academic Press: New York, 1965.
(18) Cahn, J. W.; Hilliard, J. E. *J. Chem. Phys.* **1958**, *28*, 258.
(19) de Gennes, P.-G. "Scaling Concepts in Polymer Physics"; Cornell University Press: Ithaca, NY, 1979.
(20) Verwey, E. J. W.; Overbeek, J. Th. G. "Theory of the Stability of Lyophobic Colloids"; Elsevier: Amsterdam, 1948.
(21) Long, J. A.; Osmond, S. W. J.; Vincent, B. *J. Colloid Interface Sci.* **1973**, *42*, 545.
(22) Dolan, A. K.; Edwards, S. F. *Proc. R. Soc. London A* **1975**, *343*, 417.